blood®
Regular Article

RED CELLS, IRON, AND ERYTHROPOIESIS

17(*R*)-Resolvin D1 protects against sickle cell–related inflammatory cardiomyopathy in humanized mice

Enrica Federti,[1] Domenico Mattoscio,[2,*] Antonio Recchiuti,[2,*] Alessandro Matte,[1] Maria Monti,[3,4] Flora Cozzolino,[3,4] Manuela Iezzi,[5] Martina Ceci,[5] Alessandra Ghigo,[6] Emanuela Tolosano,[6] Angela Siciliano,[1] Jacopo Ceolan,[1] Veronica Riccardi,[1] Elisa Gremese,[7,8] Carlo Brugnara,[9] and Lucia De Franceschi[1]

[1]Department of Engineering for Innovative Medicine, University of Verona and Azienda Ospedaliera Universitaria Integrata Verona, Verona, Italy; [2]Department of Medical, Oral, and Biotechnology Science; Center for Advanced Studies and Technology, G. d'Annunzio University of Chieti, Pescara, Italy; [3]Dipartimento Scienze Chimiche, Università degli studi di Napoli Federico II, Naples, Italy; [4]CEINGE Biotecnologie Avanzate Franco Salvatore, Naples, Italy; [5]Department of Medicine and Aging Science, Center for Advanced Studies and Technology, G. d'Annunzio University of Chieti, Pescara, Italy; [6]Department Molecular Biotechnology and Health Sciences, Molecular Biotechnology Center Guido Tarone, University of Torino, Torino, Italy; [7]Division of Clinical Immunology, Fondazione Policlinico Universitario A. Gemelli-Istituto di Ricovero e Cura a Carattere Scientifico, Università Cattolica del Sacro Cuore, Rome, Italy; [8]Immunology Core Facility, Fondazione Policlinico Universitario A. Gemelli-Istituto di Ricovero e Cura a Carattere Scientifico, Rome, Italy; and [9]Departments of Laboratory Medicine and Pathology, Boston Children's Hospital, Harvard Medical School, Boston, MA

KEY POINTS

- **In SS mice, unresolved inflammation initiates a cardiac hypertrophic neutrophil-driven response.**
- **Treatment with 17R-RvD1 prevents the H/R-induced pathways involved in maladaptive heart remodeling in SS mice.**

Cardiovascular disease has been recognized as the main cause of death in adults with sickle cell disease (SCD). Although the exact mechanism linking SCD to cardiomyopathy remains elusive, a possible role of subclinical acute transient myocardial ischemia during acute sickle cell–related vaso-occlusive crises (VOCs) has been suggested. We approached SCD cardiomyopathy by integrated omics using humanized SS mice exposed to hypoxia/reoxygenation (H/R; 10 hours hypoxia followed by 3 hours reoxygenation) stress, mimicking acute VOCs. In sickle cell (SS) mice exposed to H/R, a neutrophil-driven cardiac hypertrophic response is initiated by cardiac proinflammatory pathways, intersecting proteins and micro RNA involved in profibrotic signaling. This response may be facilitated by local unresolved inflammation. We then examined the effect of 17(*R*)-resolvin D1 (17R-RvD1), a member of the specialized proresolving lipid mediator superfamily, administration on H/R-activated profibrotic and proangiogenic pathways. In SS mice, we found that 17R-RvD1 (1) modulates miRNAome; (2) prevents the activation of NF-κB p65; (3) protects against the H/R-induced activation of both platelet derived growth factor receptor and transforming growth factor (TGF)-β1/Smad2-3 canonical pathways; (4) reduces the expression of hypoxia-inducible factor-dependent proangiogenic signaling; and (5) decreases the H/R-induced proapoptotic cell signature. The protective role of 17R-RvD1 against H/R-induced maladaptive heart remodeling was supported by the reduction of galectin-3, procollagen C-proteinase enhancer-1, and endothelin-1 expression and perivascular fibrosis in SS mice at 3 days after H/R stress compared with vehicle-treated SS animals. Collectively, our data support the novel role of unresolved inflammation in pathologic heart remodeling in SCD mice in response to H/R stress. Our study provides new evidence for protective effects of 17R-RvD1 against SCD-related cardiovascular disease.

Introduction

Sickle cell disease (SCD) is a severely debilitating hereditary red cell disorder.[1] Inflammatory vasculopathy and cardiopulmonary complications largely affect the quality of life of patients with SCD.[2,3] In addition, cardiovascular disease has been recognized as the main cause of death in adults with SCD.[2,4] Previous studies have shown the presence of subclinical acute transient myocardial ischemia in both young adults and children with SCD during acute vaso-occlusive crises (VOCs).[4,5] In a mouse model for SCD ("Berk" mice), Baker et al reported an upregulation of cell pathways involved in extracellular matrix remodeling, angiogenesis, and lipid metabolism.[6] Furthermore, recent evidence in both mouse models and patients with SCD links the proinflammatory cytokine interleukin-18 (IL-18) with heart remodeling, fibrosis progression, and an increase risk of ventricular arrythmias.[7-10] Of note, Niss et al reported a reduction of myocardial fibrosis in patients with SCD early treated with either chronic transfusion regimen or hydroxyurea,[11] further supporting the role of chronic inflammation in the pathogenesis of SCD cardiac pathology. Although ischemic/reperfusion damage promoting myocardial fibrosis has been suggested to contribute to SCD-related cardiomyopathy, mechanisms of disease progression are still unclear.[4,12,13]

Studies in different models of acute myocardial infarction have shown the crucial role of unresolved inflammation in myocardial damage and in progression toward heart fibrosis and heart failure.[14-17] Resolution of inflammation is an active process driven by unique specialized proresolving lipid mediators (SPMs), including resolvins (Rvs). SPMs evoke multipronged cellular and molecular responses that prevent injurious neutrophil tissue infiltration, countering inflammasome and proinflammatory mediators.[18] Through their receptors, SPMs convey acute actions to stop further inflammation and also to activate long-range molecular circuits (eg, microRNAs), beneficial in organ protection.[19] Among specialized proresolving mediators, 17(*R*)-Rv D1 (17R-RvD1) has been shown to play important protective actions in cardiovascular diseases.[20-22] Recently, we highlighted the novel contribution of abnormal proresolving events in response to ischemic/reperfusion stress in humanized sickle cell (SS) mice. The failure of acute inflammatory resolution sustains the amplified inflammatory response, making SS mice more vulnerable to inflammatory vasculopathy.[23] This may also be important in SCD-related cardiovascular disease.

Materials and methods

Design of the study

Experiments were performed on 4- to 5-month-old sex-matched (54.2% males and 45.8% females) healthy control [Hbatm1(HBA)Tow Hbbtm3(HBG1, HBB)Tow] and sickle cell [Hbatm1(HBA)Tow Hbbtm2(HBG1,HBB*)Tow] mice. The institutional animal experimental committee of University of Verona and the Italian Ministry of Health approved the experimental protocols (56DC9.64). The sample size was estimated based on previous studies using humanized SS mice.[23-28] We chose to use 4- to 5-month-old mice because, as we and others have previously reported, the sickle cell–related organ damage at this age is not severe enough to generate confounding factors when evaluating the impact of hypoxia/reoxygenation (H/R)–induced stress.[23-28] Animals with either skin lesion or hemoglobin levels <6 g/dL were excluded. A double-blind strategy was implemented to minimize potential bias in data collection. Animals were anesthetized with isoflurane and randomly assigned to experimental groups. Whole blood was collected via retro-orbital venipuncture by heparinized microcapillaries. In anesthetized perfused animals, hearts were immediately removed and divided into 2 and either immediately frozen in liquid nitrogen or fixed in 4% paraformaldehyde (overnight at 4°C). Whenever indicated, vehicle (0.5% ethanol in tap water) or 17R-RvD1 (100 ng) were administrated by gavage 1 hour before H/R, which was conducted as follow: 10 hours hypoxia (8% oxygen) and then 3 or 48 hours reoxygenation (21% oxygen).[23] To explore the possible effect of 7R-RvD1 on progression of heart, we chose the window time of 3 days after H/R and 17R-RvD1 administration, based on previous observations.[29-31] Detailed methods are reported in supplemental Materials, available on the *Blood* website.

Results

Hypoxia/reoxygenation stress increases markers of myocardial dysfunction and promotes the activation of local proinflammatory pathways

The experimental strategy we used to explore the role of H/R in the progression of sickle cell–related cardiomyopathy is based on the observations of transient ischemia associated with VOCs in patients with SCD (Figure 1A).[5] Because a previous study in another mouse model of SCD (Berk mice) excluded a role for chronic anemia in the pathogenesis of SCD-related cardiomyopathy,[6] we decide to expose SS mice to H/R stress, an established model for VOCs.[23,32] We first confirmed the presence of sickle cell–related cardiomyopathy in a humanized mouse model of SCD ("Townes" mouse strain).[7,23] We found cardiomegaly associated with (1) diastolic dysfunction with preserved systolic function, as determined by echocardiography, confirming our previous study in SS mice (supplemental Figure 1A-B; supplemental Table 1)[33]; (2) increased cardiomyocyte cross-sectional area (supplemental Figure 1C), supporting cardiomyocyte hypertrophy; (3) activation of both transcriptional factors NF-κB p65 and Nrf2, which are involved in proinflammatory and antioxidant responses, respectively (supplemental Figure 2A)[23]; and upregulation of VCAM-1 and ICAM-1, markers of inflammatory vasculopathy, and Gpx1, a cytoprotective system (supplemental Figure 2B), in the absence of heart iron accumulation (supplemental Figure 3A). This was further corroborated by higher collagen deposition in the hearts of SS mice than in the hearts of healthy animals (supplemental Figure 3B). Of note, we newly found activation of platelet-derived growth factor receptor (PDGF-R), marked by increased phosphorylation of PDGF-R (supplemental Figure 3C), which has been reported to be involved in matrix remodeling and profibrotic events in other models of hypertrophic cardiopathy (HC).[34,35]

To understand the early and late impact of H/R stress on the hearts of humanized SCD mice, we studied healthy and SS mice at 3 hours and 48 hours after 10 hours of hypoxia.[23,36] We followed the behaviors of plasma N-terminal pro B-type natriuretic peptide (NT-pro-BNP), a known marker of cardiac dysfunction and heart neutrophil infiltration, as a sign of local inflammation in response to H/R stress. Plasma NT-pro-BNP significantly increased in SCD mice at 3 hours of reoxygenation compared with either SCD mice at 48 hours of reoxygenation or healthy (AA) animals at 3 or 48 hours of reoxygenation (supplemental Figure 4A). This was paralleled by a significant increase in heart neutrophil infiltration, as determined by flow cytometry analysis, in response to hypoxia in SCD mice (supplemental Figure 4B). A higher circulating neutrophil count was also observed in SS mice after 3 hours of reoxygenation than in normoxic SS mice or healthy mice, in agreement with our previous reports[23,32] (supplemental Figure 5A). No major change in splenic neutrophils was observed in SS exposed to H/R compared with normoxic SS mice, with splenic neutrophils being higher in SS mice than healthy animals at baseline (supplemental Figure 5B). Because previous reports have linked NF-κB activation and inflammatory response in different target organs of SCD, we evaluated NF-κB in the hearts of both healthy and SS mice exposed to H/R stress.[23] SS mice displayed activation of NF-κB p65 in response to H/R stress at 3 and 48 hours after hypoxia, compared with the hearts of either normoxic SS mice or healthy animals (supplemental Figure 6A). This was associated in SS mice with the upregulation of the expression of heart endothelin-1 (ET-1) in response to H/R (supplemental Figure 6B). Of note, the expression of ET-1 was persistently higher at 48 hours after H/R in the hearts of SS mice than AA animals (supplemental Figure 6B). This is of interest because ET-1 has been shown to play a key role in (1) the progression of sickle cell–related organ damage[37,38]; and (2) both heart vascular

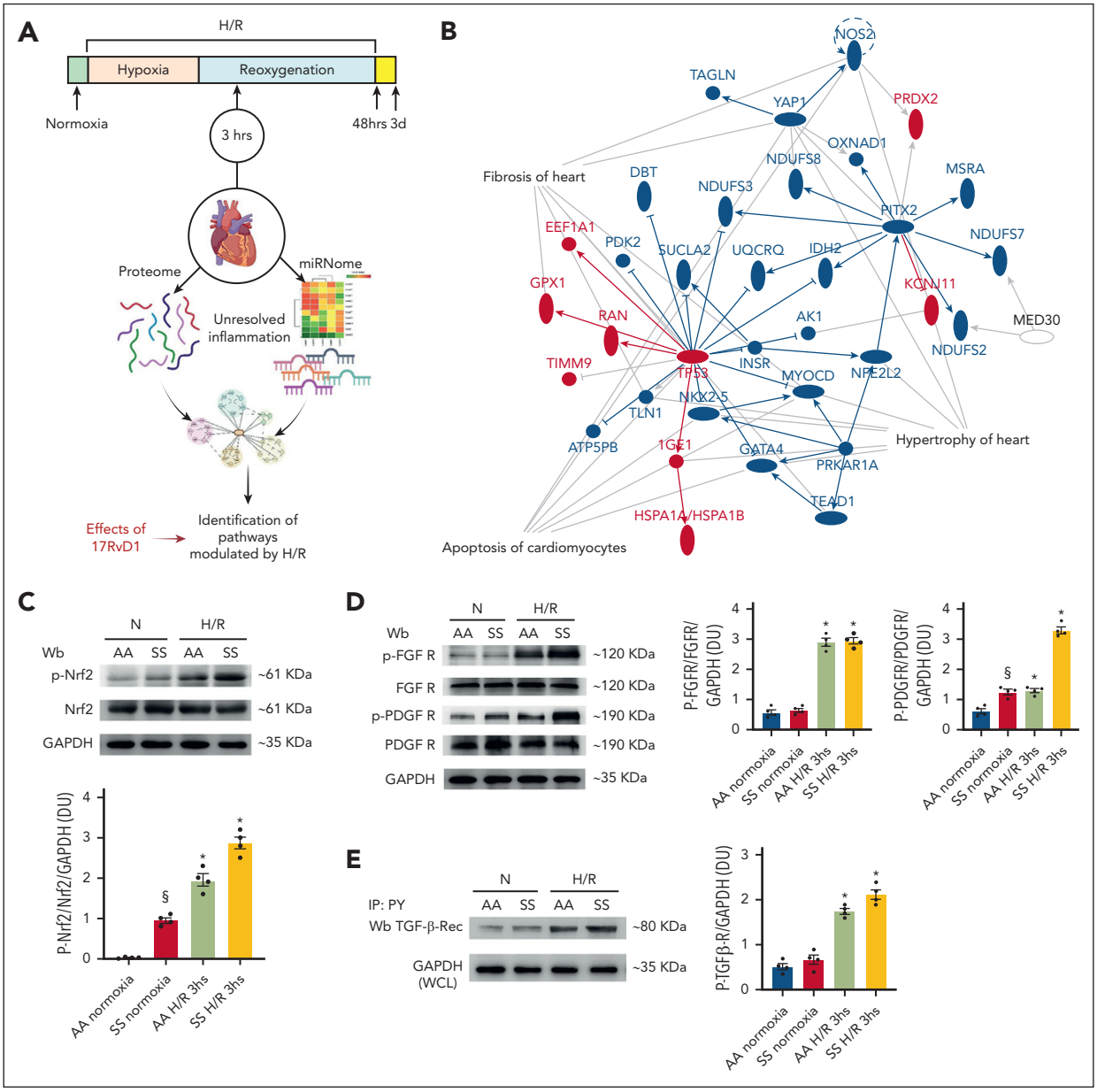

Figure 1. In sickle cell mice, heart proteomic analysis reveals that H/R stress activates proinflammatory and profibrotic pathways. (A) Schematic diagram of the experimental plan used in this study. (B) Ingenuity pathway analysis (IPA) networks generated interrogating proteins identified as differentially expressed in SS hearts under H/R stress compared with AA under H/R. The following pathways were identified as affected by H/R in the hearts of SS mice vs healthy animals: (1) fibrosis of the heart; (2) hypertrophy of the heart; and (3) apoptosis of cardiomyocytes. (C) Immunoblot analysis using specific antibodies against phosphorylated Nrf2 (p-Nrf2) and Nrf2 in the hearts of AA and SS mice in normoxia (N) and exposed to H/R: hypoxia (8% oxygen; 10 hours), followed by reoxygenation (21% oxygen; 3 hours). A total of 75 μg/μL of protein loaded on an 8% T, 2.5% C polyacrylamide gel. Glyceraldehyde 3-phosphate dehydrogenase (GAPDH) serves as protein loading control. One representative gel from 4 with similar results is shown. Densitometric analysis of immunoblots is shown (right). Data are presented as means ± standard error of the mean (SEM; n = 4). §P < .05 (compared with AA normoxia); *P < .05 (compared with normoxia by 1-way analysis of variance [ANOVA]). (D) Immunoblot analysis, using specific antibodies against phosphorylated FGF receptor (p-FGF-R), FGF-R, p-PDGF-R-B, and PDGFR-B, in the hearts of AA and SS mice. A total of 75 μg/μL of protein loaded on an 8% T, 2.5% C polyacrylamide gel. GAPDH serves as protein loading control. One representative gel from 4 with similar results is shown. Densitometric analysis of immunoblots is shown (right). Data are presented as mean ± SEM (n = 4). §P < .05 (compared with AA normoxia); *P < .05 (compared with normoxia by 1-way ANOVA). (E) Immunoprecipitation (IP) from the hearts of AA and SS mice, treated similar to panel D, using specific anti–phospho-tyrosine (PY) antibodies (IP: PY), revealed with specific anti–TGF-β receptor (TGF-β-Rec) antibody (75 μg/μL of protein loaded on an 8% T, 2.5% C polyacrylamide gel). GAPDH in whole cell lysate (WCL) is used as loading controls. One representative gel from 4 others with similar results is presented. Data are presented as means ± SEM (n = 4). *P < .05 (compared with normoxia by t test). TGF, transforming growth factor; Wb, Western blot.

endothelial dysfunction and remodeling.[39-42] Noteworthy, in SS mice exposed to hypoxia followed by 3 hours of reoxygenation, we observed increased expression of NLRP3 inflammasome (supplemental Figure 6C), which has been reported to participate in inflammasome activation in the progression of HC.[43]

Taken together, these data indicate that SS mice develop a more rapid and intense inflammatory response to H/R than healthy mice, supporting a local and amplified systemic inflammatory response to H/R stress, which is used to mimic acute VOCs in humanized SS mice.

Integrated heart proteomic and miRNA network analysis reveals the molecular features of fibrosis in pathogenesis of sickle cell–related cardiomyopathy

To decode the complexity of the pathogenesis of SCD cardiomyopathy, we sought to define a molecular signature underlying the development of cardiovascular complications with omics strategies. The semiquantitative proteomic analysis of hearts from AA and SS mice exposed to H/R identified 139 changeable proteins. We found 62 upregulated (fold change > 1.41) and 77 downregulated (fold change < 0.71) proteins in the hearts of SS mice compared with healthy animals. Proteomic data were further analyzed using the Ingenuity Pathway Analysis tool, allowing for the identification of the following pathways affected by H/R in the hearts of SCD mice vs healthy animals: (1) fibrosis of the heart; (2) hypertrophy of the heart; and (3) apoptosis of cardiomyocytes (Figure 1B). We validated the analysis by using an immunoblot approach to examine the identified key hubs. In the hearts of SS mice exposed to H/R stress, we found activation of Nrf2, a transcription factor involved in acute phase response, compared with the hearts of either normoxic SS mice or healthy animals exposed to H/R (Figure 1C). This was associated with increased heart protein oxidation evaluated by Oxyblot in H/R-exposed SS mice (supplemental Figure 7A). In agreement, we found upregulation of cytoprotective and antioxidant systems, such as heme oxygenase-1 (HO-1), Gpx-1, Nqo1, peroxiredoxin-2 (Prx2), and Prx3 (supplemental Figure 7B), in SS mice exposed to H/R stress compared with the hearts of either normoxic SS mice or healthy animals exposed to H/R stress. Examining the modulation of profibrotic pathways, we found H/R-induced activation of both FGF-B and of PDGF-B receptors, which have been reported to play a crucial role in extracellular matrix remodeling and in the development of hypertrophic cardiomyopathy[34,35,44] (Figure 1D). This was associated with the activation of transforming growth factor (TGF)-β system in SS mice exposed to H/R stress compared with healthy animals (Figure 1E).

Because the identified pathways intersected microRNAs involved in cardiovascular diseases, such as miR-25-3p, miR-16-5p, and miR-208a-3p,[45] we first evaluated the expression of these micro RNAs (miRNA)s in the hearts of SS and AA mice exposed to H/R stress. As shown in Figure 3A, we found increased expression of miR-25-3p and miR-16-5p in SS mice under normoxia compared with AA normoxic animals. H/R stress significantly increased miR-25-3p and miR-16-5p, whereas it reduced miR-208a-3p expression in the hearts of SS mice compared with healthy animals (Figure 3A). No major differences were observed in miR-208a-3p expression between these mouse strains under normoxia (Figure 2A). Thus, these results indicate that SS mice had a different heart miRNA profile compared with AA animals, and H/R stress modifies the expression of microRNAs in the heart in a selective manner. Based on these data, we extended the analysis to a panel of >90 miRNAs. As shown in Figure 2B-C, the array analysis revealed that miR-486-5p, 122-5p, 144-3p, 7a-5p,18a-5p, and 451a were significantly increased after H/R in SS mice compared with AA animals. In contrast, miR-206-3p was the only microRNA significantly downregulated in SS compared with healthy mice. By superimposing proteins and miRNAs identified from respective analyses, we found 17 dysregulated proteins among the 673 targeted by differentially expressed miRNAs and the 139 defined by proteomic analysis (Figure 2D; supplemental Figure 8A). These were found to be functionally associated with pathways involved in cardiac fibrosis, cardiac arrhythmia, and heart enlargement (Figure 2D; supplemental Figure 8A),[46-50] suggesting that the pathogenesis of sickle cell cardiomyopathy may not be related to a single pathway but to the abnormalities of several pathways. Indeed, we observed activation of vascular endothelial growth factor A (VEGF-A) receptor in the hearts of SS mice exposed to H/R compared with the hearts of either normoxic SS mice or H/R AA animals (supplemental Figure 7B). This was associated with upregulation of VEGF-A in SS mice vs AA mice exposed to H/R, whereas the expression of angiopoietin-2 was higher in the hearts of mouse strains exposed to H/R stress than in normoxic animals (supplemental Figure 7B). No major changes in the heart expression of angiopoietin-1 under different conditions were observed (supplemental Figure 8B).

Collectively, these data indicate that, in SS mice, the H/R stress contributes to a sustained activation of multiple NF-κB–dependent pathways that include both miRNAs and proteins converging in modulation of profibrotic and cardiac-remodeling pathways.

Treatment with 17R-RvD1 protects against the progression of inflammatory-related cardiovascular disease and modulates miRNA targeting cardiac profibrotic pathways

In SCD, the observed relentless inflammatory damage might be favored by the lack of cardiac proresolving mechanisms during sickle cell–related acute events. Therefore, we set out to determine whether treatment with 17R-RvD1 could reduce the burden of SCD heart disease. 17-RvD1–treated SS mice exhibited a significant smaller reduction in functional shortening after H/R stress than vehicle-treated SS animals, suggesting a role of 17R-RvD1 in maintaining cardiac contractility during H/R stress (Figure 3A; supplemental Table 2). In addition, 17R-RvD1–treated SS mice exposed to H/R displayed reduced (1) atrial natriuretic peptide heart expression, a marker of myocardial dysfunction; (2) serum and heart expression of galectin-3 (Gal-3), involved in maladaptive cardiac remodeling[51-53] (Figure 3B-C; supplemental Figure 9A); and (3) heart neutrophil infiltration (Figure 3D), compared with vehicle-treated animals. We also noted increased proresolving CD206-polarized intracardiac neutrophils, identified as $Ly6G^+$ $CD206^+$ cells, in 17R-RvD1 SS mice exposed to H/R compared with vehicle-treated animals (Figure 3E). This was associated with a reduction in H/R-induced heart activation of NF-κB p65, which is supported by the following: (1) a decrease in nuclear localization of phospho–NF-κB p65, as defined with DAPI (4′,6-diamidino-2-phenylindole) and the mean nuclear phospho–NF-κB p65 fluorescence intensity (Figure 4A; left panel, immunomicroscopy; supplemental Figure 9B); and (2) a decrease in the amount of NF-κB p65 phospho-form, by immunoblot analysis (Figure 4A, right panel). In agreement, we found downregulation of markers of inflammatory vasculopathy, such as P-selectin, thromboxane synthase, and ET-1 (Figure 4B), as well as in NLRP3 in the hearts from 17R-RvD1–treated SS mice exposed to H/R compared with vehicle-treated animals (Figure 4C). In agreement, we found a reduction of NLRP3 inflammasome signaling, resulting in decreased caspase-1 activation and downregulation of *IL-1b* and *IL-18* gene expression in the hearts of 17R-RvD1–treated SS

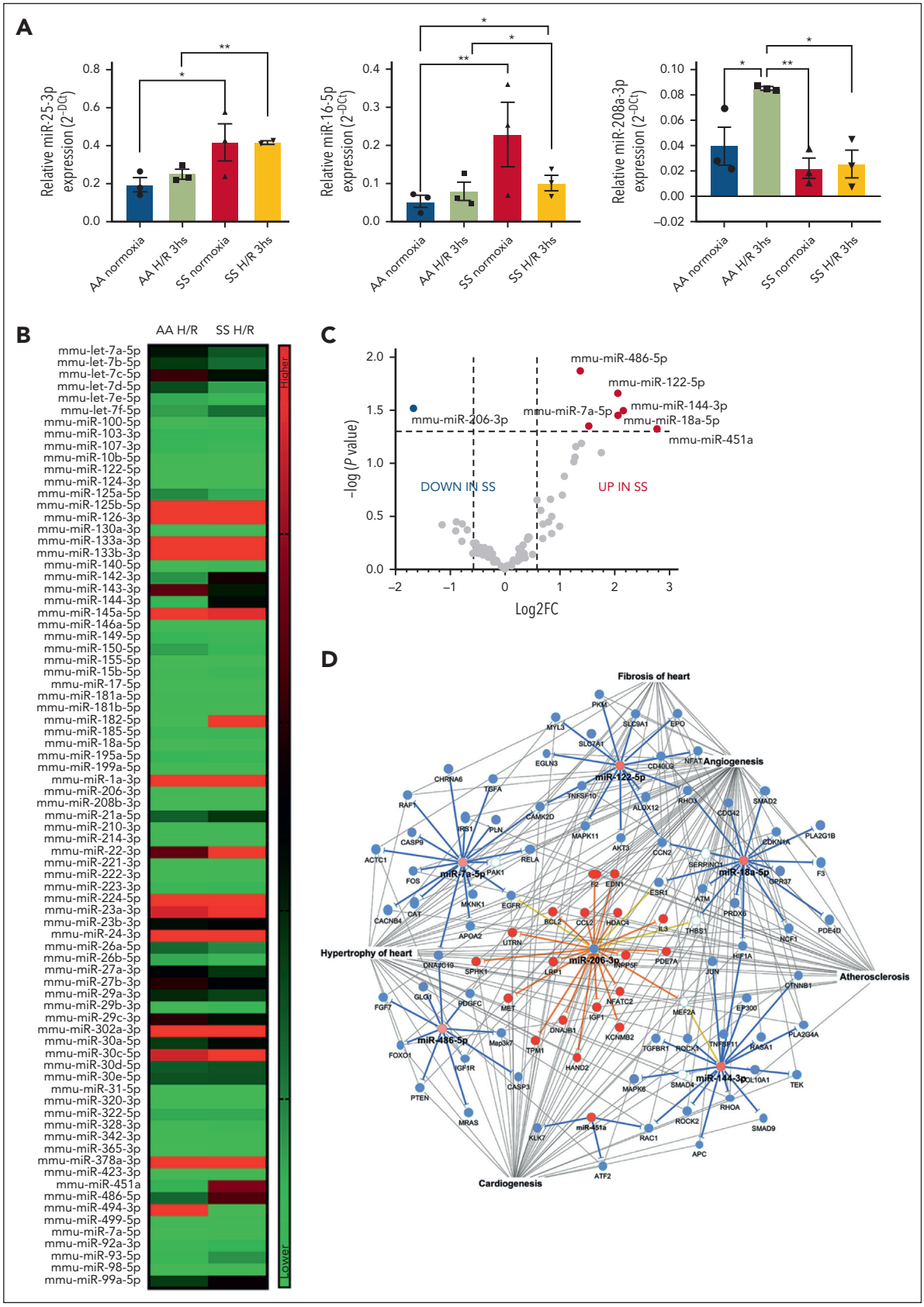

Figure 2. Hypoxia/reoxygenation stress modulates microRNAs in the hearts of sickle cell mice. (A) Relative expression of microRNAs from the hearts obtained from AA or SS mice under normoxia or H/R conditions. Expression of miRNAs was determined with quantitative polymerase chain reaction and normalized using U6SNRNA, RNU5G, RNU1A1, and SNORD61 as housekeeping small noncoding RNAs. Results are mean ± SEM from 3 separate mice. *$P < .05$; **$P < .01$ (1-way ANOVA). (B-C) Heat map and volcano plot showing fold change (FC) in the relative expression of miRNAs in the hearts of AA and SS mice under H/R compared with normoxia. Expression of microRNAs was

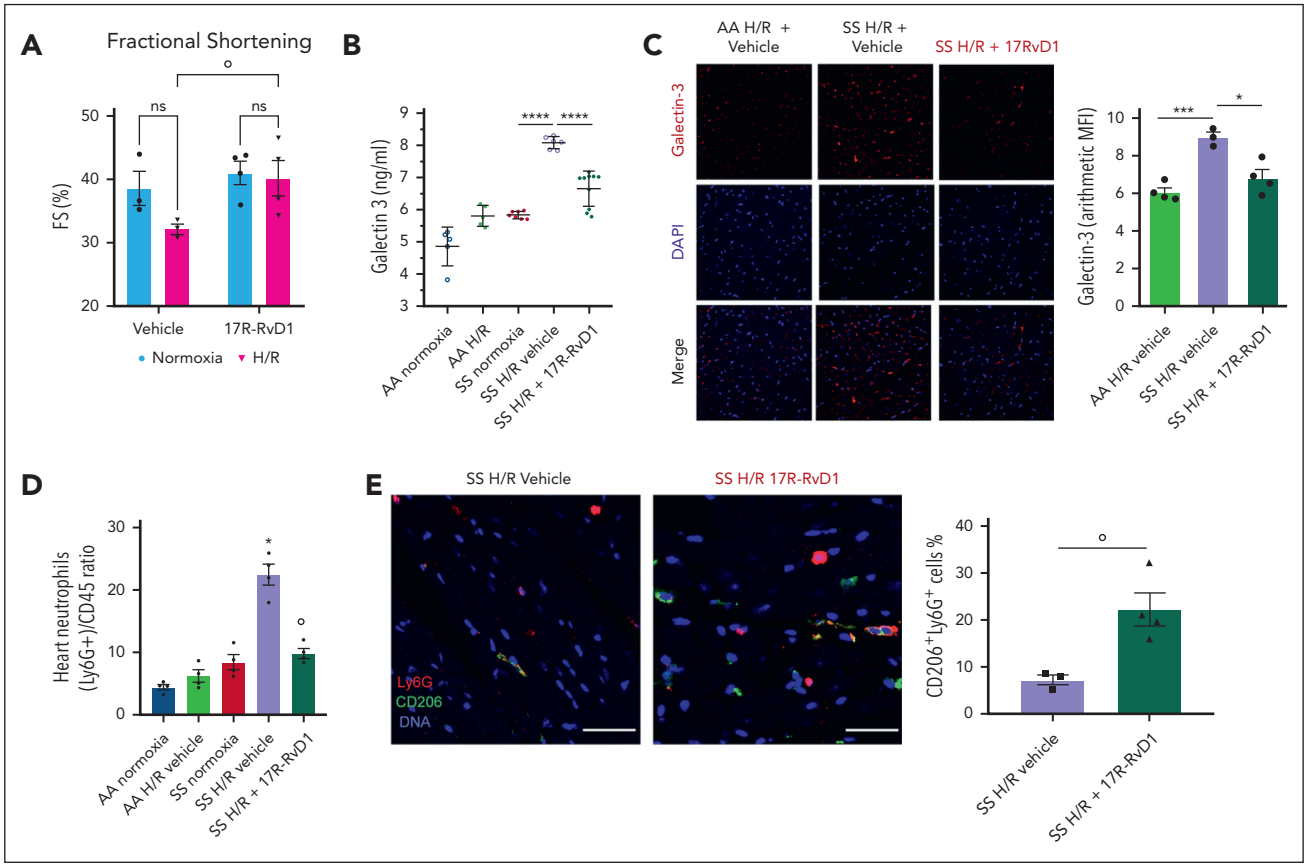

Figure 3. In sickle cell mice, 17R-RvD1 preserves cardiac contractility and protects against H/R-induced neutrophil heart infiltration. (A) Fractional shortening (FS [%]) in SS mice under normoxia and exposed to H/R stress and treated with either vehicle or 17R-RvD1 (n = 3-4); $P < .05$ (compared with vehicle-treated H/R SS mice). (B) Serum Gal-3 from AA and SS mice under normoxia and treated with vehicle or 17R-RvD1. Data are presented as mean ± SEM (n = 5-9). $^{****}P < .005$ (by unpaired t test with Welch correction). (C) Immunofluorescence expression of Gal-3 (red) in heart microsections from AA mice and SS mice exposed to H/R stress treated with either vehicle or 17R-RvD1. Nuclei (blue) were stained with DAPI. Quantification of Gal-3 was performed on 3 to 4 samples per group (6 × 400 field per sample) with ZEN 2.3 Software. Data are presented as mean ± SEM (n = 3-4). $^{*}P < .05$; $^{***}P < .001$ (by 1-way ANOVA). (D) Heart neutrophils infiltration identified, by flow cytometric analysis, as $CD45^{+}Ly6G^{+}$ cells from AA and SS mice under normoxia and treated with vehicle or 17R-RvD1 (100 ng) and exposed to H/R: hypoxia (8% oxygen; 10 hours), followed by reoxygenation (21% oxygen; 3 hours). Data are presented as mean ± SEM (n = 4). $^{*}P < .05$ (compared with normoxia); $^{\circ}P < .05$ (compared with vehicle-treated H/R SS mice by 1-way ANOVA). (E) One representative image by immunomicroscopy (left) and quantification (right) of proresolving CD206-polarized intracardiac neutrophils (per mm^2 heart tissue) identified by double immunofluorescence for Ly6G and CD206 in SS mice exposed to H/R and treated with vehicle or 17R-RvD1. Data are presented as mean ± SEM (n = 3-4). $^{\circ}P < .05$ (compared with vehicle-treated H/R SS mice by t test; size scale bar, 40 μm). MFI, mean fluorescence intensity.

mice exposed to H/R compared with vehicle-treated animals (supplemental Figure 10A-B).

We also explored the response of Nrf2 in the hearts of SS mice exposed to H/R stress and treated with 17R-RvD1. As shown in Figure 5A, 17R-RvD1 prevented the activation of Nrf2 in the hearts of SS mice compared with vehicle-treated animals. Consistent with this observation, we found reduced oxidation of proteins in the hearts of SS mice exposed to H/R stress (supplemental Figure 10D). This was associated with the downregulation of Nrf2-dependent cytoprotective systems, such as HO-1 and Nqo1, as well as other antioxidants such as Prx2 and Prx3 (Figure 5B-C).

Because we and others previously reported that Rvs reduce NF-κB activation by modulation of microRNAs,[23,54] we determined the effects of 17R-RvD1 on the expression of miRNAs that we found to be modified in SS hearts during H/R. As shown in Figure 5D, 17R-RvD1 reduced miR-25-3p, 16-5p, and 144-3p, which were upregulated by H/R, whereas it increased miR-206-3p and further reduced 208-3p, which was suppressed by H/R. In contrast, miR-18a-5p, 122-5p, 451a, 486-5p, and 7a-5p were not modified by 17R-RvD1 (supplemental Figure 11A). To highlight 17R-RvD1–driven proresolving signaling and its biological significance, we determined the intersections between 17R-RvD1–regulated miRNAs and their relative targets with the identified proteins, along with their associated pathophysiological functions (supplemental Figure 11B). 17R-RvD1–regulated miRNAs targeted 418 proteins. Of them, 13 was among the proteins identified by our proteomic analysis and linked to cardiac dysfunctions, such as HC (supplemental Figure 11B).[46-50,55,56]

Figure 2 (continued) determined (from n = 5 mice per condition). Dotted lines in the volcano plot represents cutoff values for significant ($P < .05$) differentially expressed ($-0.58 > \log_2 FC > 0.58$) in SS hearts under H/R compared with AA hearts under H/R. (D) IPA networks generated interrogating proteins targets of differentially expressed miRNAs in SS hearts under H/R stress.

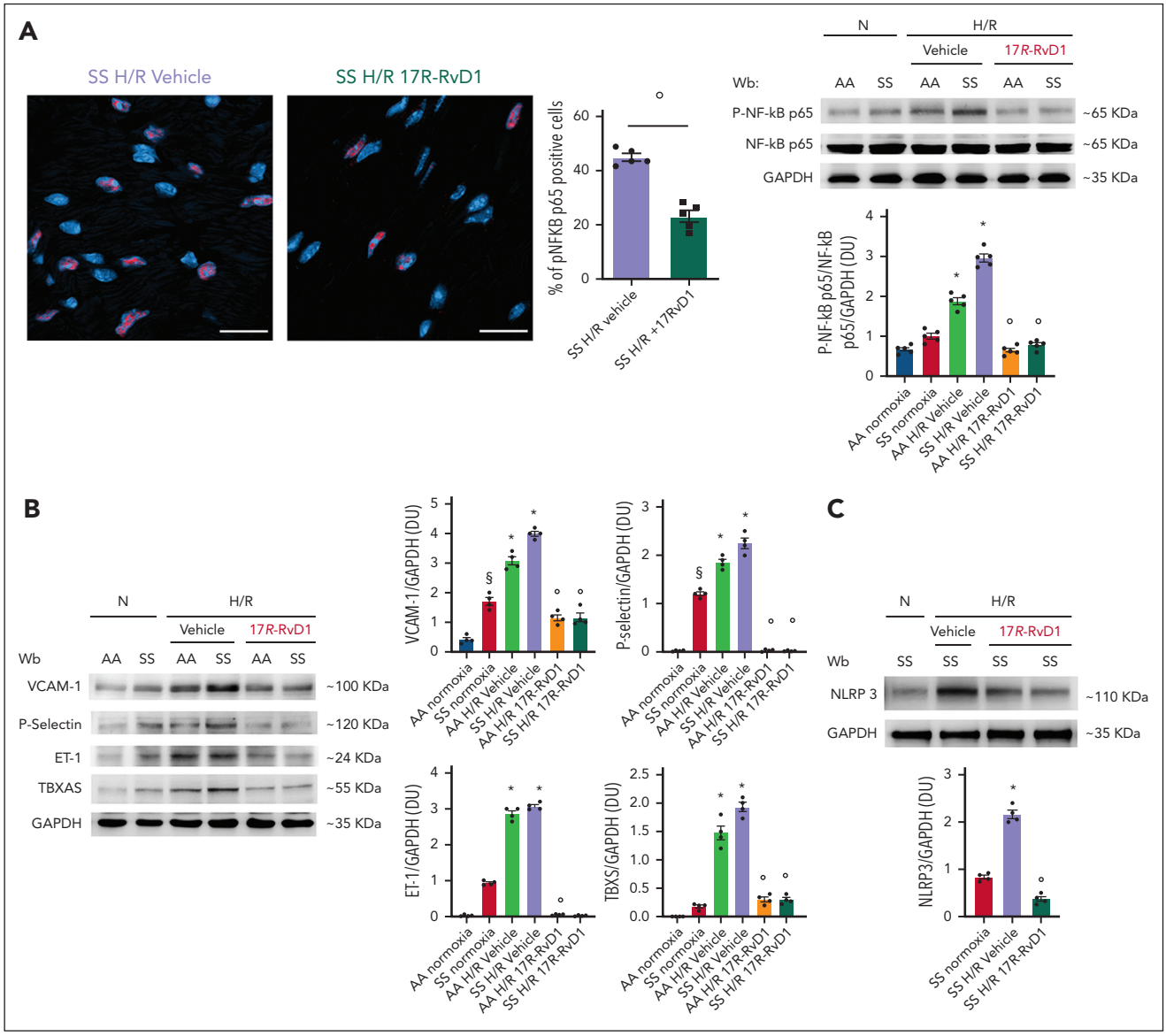

Figure 4. 17R-RvD1 prevents the activation of NF-κB–dependent pathways and reduces NLRP3 inflammasome. (A) Activated phosphorylated NF-κB p65 (p-NF-κB p65) in heart cells identified with immunofluorescence staining (size scale bar, 20 μm) in SS mice exposed to H/R stress and treated with either vehicle or 17R-RvD1 (left). Data are presented as mean ± SEM (n = 5). °P < .05 (compared with vehicle-treated H/R SS mice by t test). Quantification of total NF-κB in heart cells is shown in supplemental Figure 8B. Immunoblot analysis (right), using specific antibodies against p-NF-κB p65 and NF-κB p65, of heart from AA and SS mice under normoxia and treated with vehicle or 17R-RvD1 (100 ng) and exposed to H/R: hypoxia (8% oxygen; 10 hours), followed by reoxygenation (21% oxygen; 3 hours). A total of 75 μg/μL of protein loaded on an 8% T, 2.5% C polyacrylamide gel. Glyceraldehyde 3-phosphate dehydrogenase (GAPDH) serves as protein loading control. One representative gel from 4 with similar results is shown. Densitometric analysis of immunoblots is shown (right). Data are presented as means ± SEM (n = 4). *P < .05 (compared with normoxia); °P < .05 (compared with vehicle-treated mice by 1-way ANOVA). (B) Immunoblot analysis, using specific antibodies against P-selectin, ET-1, and thromboxane synthase (TBXS), in the hearts of AA and SS mice treated. A total of 75 μg/μL of protein loaded on an 11% T, 2.5% C polyacrylamide gel. GAPDH serves as protein loading control. One representative gel from 4 with similar results is shown. Densitometric analysis of immunoblots is shown (right). Data are presented as means ± SEM (n = 4). *P < .05 (compared with normoxia); §P < .05 (compared with AA normoxia); °P < .05 (compared with vehicle-treated mice by 1-way ANOVA). (C) Immunoblot analysis, using specific antibodies against NLRP3, in the hearts of AA and SS mice, treated similar to panel B. A total of 75 μg/μL of protein loaded on an 8% T, 2.5% C polyacrylamide gel. GAPDH serves as protein loading control. One representative gel from 4 with similar results is shown. Densitometric analysis of immunoblots is shown (lower). Data are presented as means ± SEM (n = 4). *P < .05 (compared with normoxia); °P < .05 (compared with vehicle-treated mice). Wb, Western blot.

In sickle cell mice exposed to H/R stress, 17R-RvD1 prevents the activation of pathways involved in maladaptive heart remodeling

Previous studies in other models of heart diseases have reported that Rvs protect against profibrotic stimuli.[20,57] Here, we show that 17R-RvD1 protects against the H/R-induced activation of both fibroblast growth factor (FGF)-B and PDGF-B receptors (Figure 6A; supplemental Figure 12A) and downregulates fibronectin-1 gene expression (Supplementary 12Sb), which plays a key role profibrotic events after H/R stress.[56] This was associated with a reduction in the activation of TGF-β canonical pathway toward Smads[58] (Figure 6B). Indeed, we found reduced activation of Smad2/3 (as phospho-Smad2/3) and downregulation of Smad4, associated with upregulation of the feedback inhibitor Smad7, in the hearts of 17R-RvD1–treated SS mice (Figure 6C; supplemental Figure 12C).

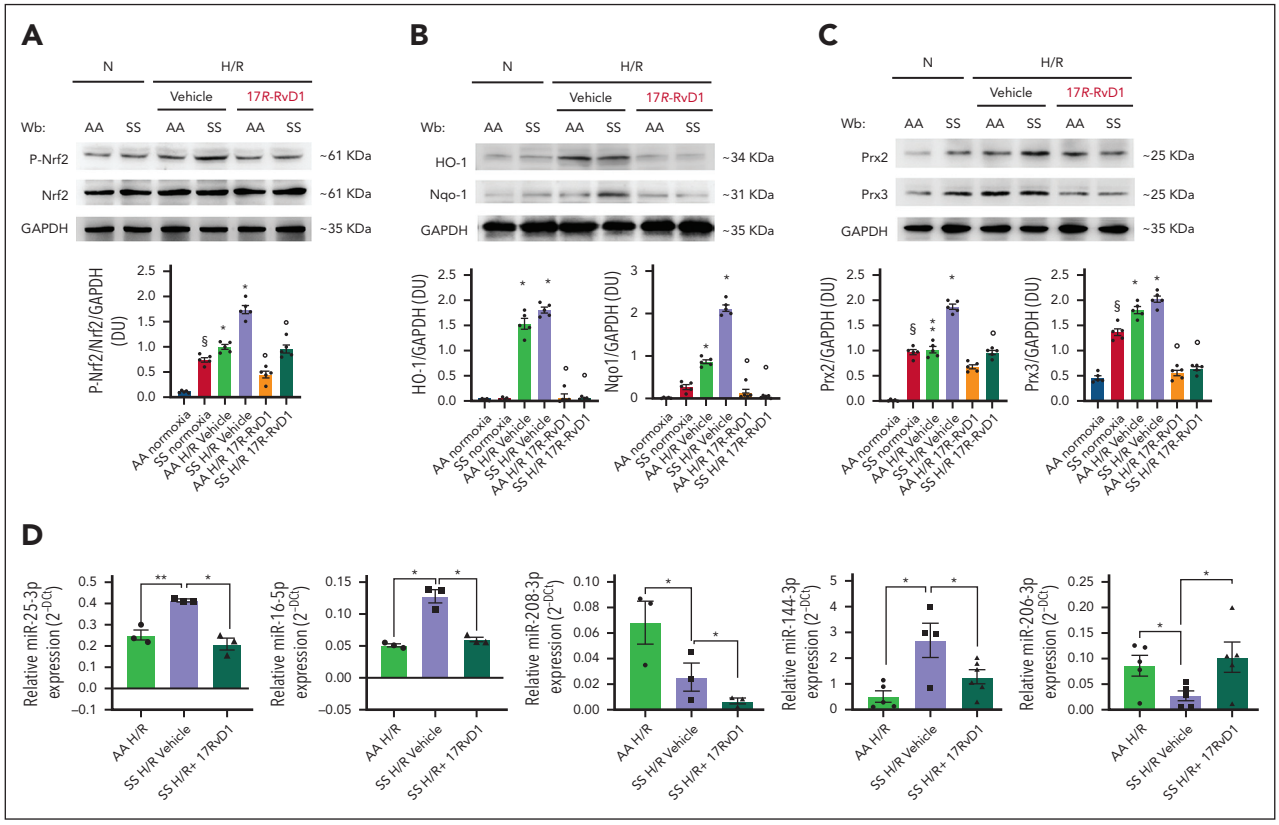

Figure 5. 17R-RvD1 prevents H/R-induced activation of Nfr2 system and modulates miRNA related to proinflammatory and profibrotic pathways in the hearts of sickle cell mice. (A) Immunoblot analysis using specific antibodies against p-Nrf2 and Nrf2 in the hearts of AA and SS mice under normoxia and treated with vehicle or 17R-RvD1 (100 ng) and exposed to H/R: hypoxia (8% oxygen; 10 hours), followed by reoxygenation (21% oxygen; 3 hours); 75 μg/μL of protein loaded on an 8% T, 2.5% C polyacrylamide gel. One representative gel from 4 gels with similar results is shown. Densitometric analysis of immunoblots is shown on the right. Data are presented as means ± SEM (n = 4). *P < .05 (compared with normoxia); §P < .05 (compared with AA normoxia); °P < .05 (compared with vehicle-treated mice). (B) Immunoblot analysis using specific antibodies against HO-1 and Nqo1 in the hearts of AA and SS mice treated, similar to panel A; 75 μg/μL of protein loaded on an 11% T, 2.5% C polyacrylamide gel. Glyceraldehyde 3-phosphate dehydrogenase (GAPDH) serves as protein loading control. One representative gel from 4 with similar results is shown. Densitometric analysis of immunoblots is shown (right). Data are presented as means ± SEM (n = 4). *P < .05 (compared with normoxia); °P < .05 (compared with vehicle-treated mice by 1-way ANOVA). (C) Immunoblot analysis, using specific antibodies against Prx2 and Prx3, in the hearts of AA and SS mice treated similar to panel A; 30 μg/μL of protein loaded on an 11% T, 2.5% C polyacrylamide gel. GAPDH serves as protein loading control. One representative gel from 4 with similar results is shown. Densitometric analysis of immunoblots is shown (right). Data are presented as means ± SEM (n = 4). *P < .05 (compared with normoxia); §P < .05 (compared with AA normoxia); °P < .05 (compared with vehicle-treated mice by 1-way ANOVA). (D) miRNAs regulated by 17R-RvD1 in the hearts of SS mice undergoing H/R. MicroRNA expression was determined using RNU5G, RNU1A1, and SNORD61 as housekeeping small noncoding RNAs. *P < .05; **P < .01 (1-way ANOVA). Wb, Western blot.

In SS mice exposed to H/R stress, we also observed a significant decrease in H/R-induced upregulation of hypoxia-inducible factor (HIF)1a and HIF2 (Figure 6D), reduced activation of VEGF-R, and downregulation in heart VEGF-A and angiopoietin-2 expression, compared with vehicle-treated mice (Figure 6E; supplemental Figure 13A). This was also confirmed by immune-microscopy, showing that 17R-RvD1 completely abolished the H/R-induced upregulation of VEGF-R both in small and large heart vessels (evaluated by $CD31^+$ staining for vascular endothelial cells) in SS mice (Figure 6E, right panel; supplemental Figure 13B). No change in angiopoietin-1 expression was observed within the different groups (Figure 6E; supplemental Figure 13A). Overall, these studies provide in vivo evidence that 17R-RvD1 treatment protects SS mice against H/R-induced heart injury by suppressing key mediators of neoangiogenesis and maladaptive cardiovascular remodeling. The protective role of 17-RvD1 was also supported by the following: (1) the reduction of both serum Gal-3 and procollagen C-proteinase enhancer-1, a marker of collagen maturation[53,59,60]; (2) the persistent downregulation of ET-1 expression; and (3) perivascular fibrosis (alpha smooth muscle actin [a-SMA] staining), associated with a trend toward reduction of collagen heart deposition in SS mice treated with 17-RvD1, compared with vehicle-treated SS animals at 3 days after H/R (Figure 7A-C; supplemental Figure 14A-B). Of note, perivascular fibrosis initially characterizes heart reactive fibrosis and has been linked to vascular endothelial dysfunction.[53,61] ET-1, known to promote vascular dysfunction, is one of the triggers of perivascular fibrosis.[40,62-65]

In sickle cell mice, 17R-RvD1 protects the heart from hypoxia/reoxygenation-induced ER stress

Progression of cardiovascular diseases such as cardiac hypertrophy has been recently linked to sustained endoplasmic reticulum (ER) stress, resulting in the activation of unfolded protein response (UPR) system.[66-69] In SCD mice exposed to H/R, 17R-RvD1 prevented the activation of the UPR system, as supported by the downregulation of activating transcription factor (ATF)6, ATF4, and C/EBP homologous protein (CHOP) (Figure 7D). We found a decrease of apoptotic markers, including not only CHOP and GADD34 but also caspase-3, determined by both

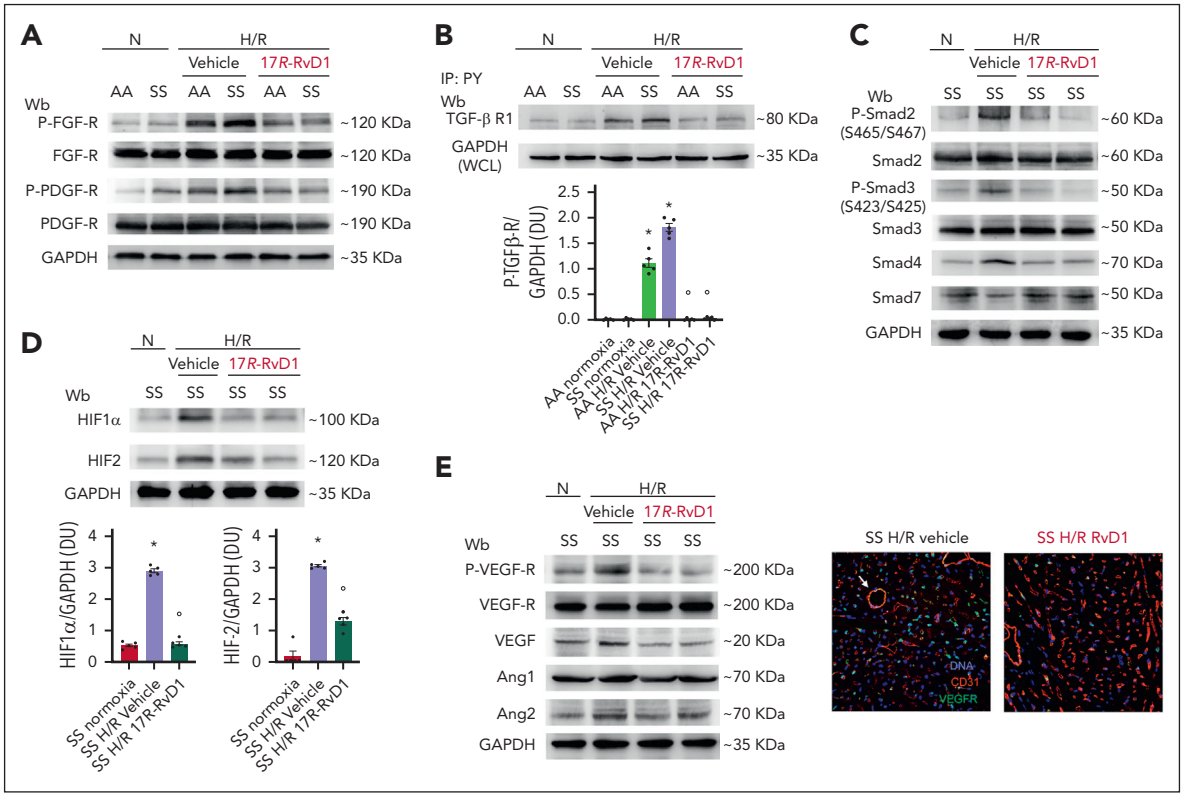

Figure 6. 17R-RvD1 protects against the H/R activation of profibrotic pathways in sickle cell mice. (A) Immunoblot analysis using specific antibodies against p-FGF-R, FGF-R, p-PDGF-R, and PDGF-R in the hearts of AA and SS mice under normoxia, treated with vehicle or 17R-RvD1 (100 ng), and exposed to H/R: hypoxia (8% oxygen; 10 hours), followed by reoxygenation (21% oxygen; 3 hours). One representative gel from 4 gels with similar results is shown; 75 μg/μL of protein loaded on an 11% T, 2.5% C polyacrylamide gel. Glyceraldehyde 3-phosphate dehydrogenase (GAPDH) serves as protein loading control. Densitometric analysis immunoblots are shown in supplemental Figure 12A. (B) IP of the hearts of AA and SS mice, treated similar to panel A, using specific IP: PY, revealed with specific anti–TGF-β Rec antibody (75 μg/μL of protein loaded on an 8% T, 2.5% C polyacrylamide gel). GAPDH in WCL is used as loading controls. One representative gel from 4 others with similar results is presented. Densitometric analysis of immunoblots is shown (lower panel). Data are presented as means ± SEM (n = 4). *P < .05 (compared with normoxia); °P < .05 (compared with vehicle-treated mice by 1-way ANOVA). (C) Immunoblot analysis using specific antibodies against phosphorylated Smad2 (p-Smad2), Smad2, p-Smad3, Smad3, Smad4, and Smad7 in the hearts of AA and SS mice under normoxia, treated with vehicle or 17R-RvD1 (100 ng), and exposed to H/R: hypoxia (8% oxygen; 10 hours), followed by reoxygenation (21% oxygen; 3 hours). One representative gel from 4 gels with similar results is shown. A total of 75 μg/μL of protein loaded on an 11% T, 2.5% C polyacrylamide gel. GAPDH serves as protein loading control. Densitometric analysis immunoblots are shown in supplemental Figure 12C. (D) Immunoblot analysis using specific antibodies against HIF1α and HIF2 in the hearts of AA and SS mice treated similar to panel C. One representative gel from 4 gels with similar results is shown; 50 μg/μL of protein loaded on an 8% T, 2.5% C polyacrylamide gel. GAPDH serves as protein loading control. Densitometric analysis of immunoblots is shown in the lower panel. Data are presented as means ± SEM (n = 4). *P < .05 (compared with normoxia); °P < .05 (compared with vehicle-treated mice by 1-way ANOVA). (E) Immunoblot analysis (left) using specific antibodies against phosphorylated VEGF receptor (p-VEGF-R), VEGF-R, angiopoietin-1 (Ang 1), and Ang 2 in the hearts of AA and SS mice treated similar to panel C. One representative gel from 4 gels with similar results is shown; 75 μg/μL of protein loaded on a 10% T, 2.5% C polyacrylamide gel. GAPDH serves as protein loading control. Densitometric analysis of immunoblots is shown in supplemental Figure 13A. Data are presented as means ± SEM (n = 4). *P < .05 (compared with normoxia). °P < .05 (compared with vehicle-treated mice by 1-way ANOVA). Representative merged immunofluorescence staining of VEG-FR on small and large CD31$^+$ vascular endothelial cells in the hearts of SS mice undergoing H/R and treated with vehicle or 17R-RvD1 (right). Arrow denotes a large blood vessel staining positive for VEGF-R. Nuclei were stained with DAPI. Separate staining is shown in supplemental Figure 13B. Wb, Western blot.

procaspase-to-cleaved caspase-3 ratio and caspase 3 staining in the hearts of 17R-RvD1–treated SS mice exposed to H/R, compared with vehicle-treated animals (Figure 7E; supplemental Figure 14C). Collectively, these data indicate that 17R-RvD1 mitigates H/R-induced acute heart stress, resolves the related amplified inflammation and vascular dysfunction, and prevents the activation of profibrotic mechanism.

Discussion

Here, we show that acute inflammatory events triggered by H/R stress remain unresolved in the hearts of SS mice, promoting the activation of cardiac proinflammatory pathways that intersect proteins and miRNAs involved in profibrotic signaling.[70-75] This is extremely interesting because growing evidence in different heart disorders supports the key contribution of unresolved inflammation in worsening myocardial repair events after H/R stress.[15,16] In our study, the beneficial effects of 17R-RvD1 support the role of impaired proresolving events in the pathogenesis of sickle cell–related cardiomyopathy. Indeed, 17R-RvD1 maintains cardiac contractility and protects SS mice against H/R-induced heart neutrophil infiltration and overactivation of NF-κB pathways, which intersect miR-25-3p, -16-5p, and -144-3p and the NLRP3 inflammasome. Of note, in SS mice, 17R-RvD1 treatment increases the amount of heart CD206$^+$ neutrophils that assist the resolution of inflammation and tissue repair after H/R stress.[21,76-78] The key role of RvD1 in skewing immune cell phenotype to promote the resolution of inflammation has been reported in models of heart failure.[21] In addition, the ability of Rv to shift neutrophil plasticity is being recently uncovered in different diseases.[18,79] Therefore, our results corroborate the twofold actions of 17R-RvD1 on peripheral and local heart neutrophils (namely, prevention of excessive recruitment and promotion of a proresolving phenotype shift). This agrees with (1) the

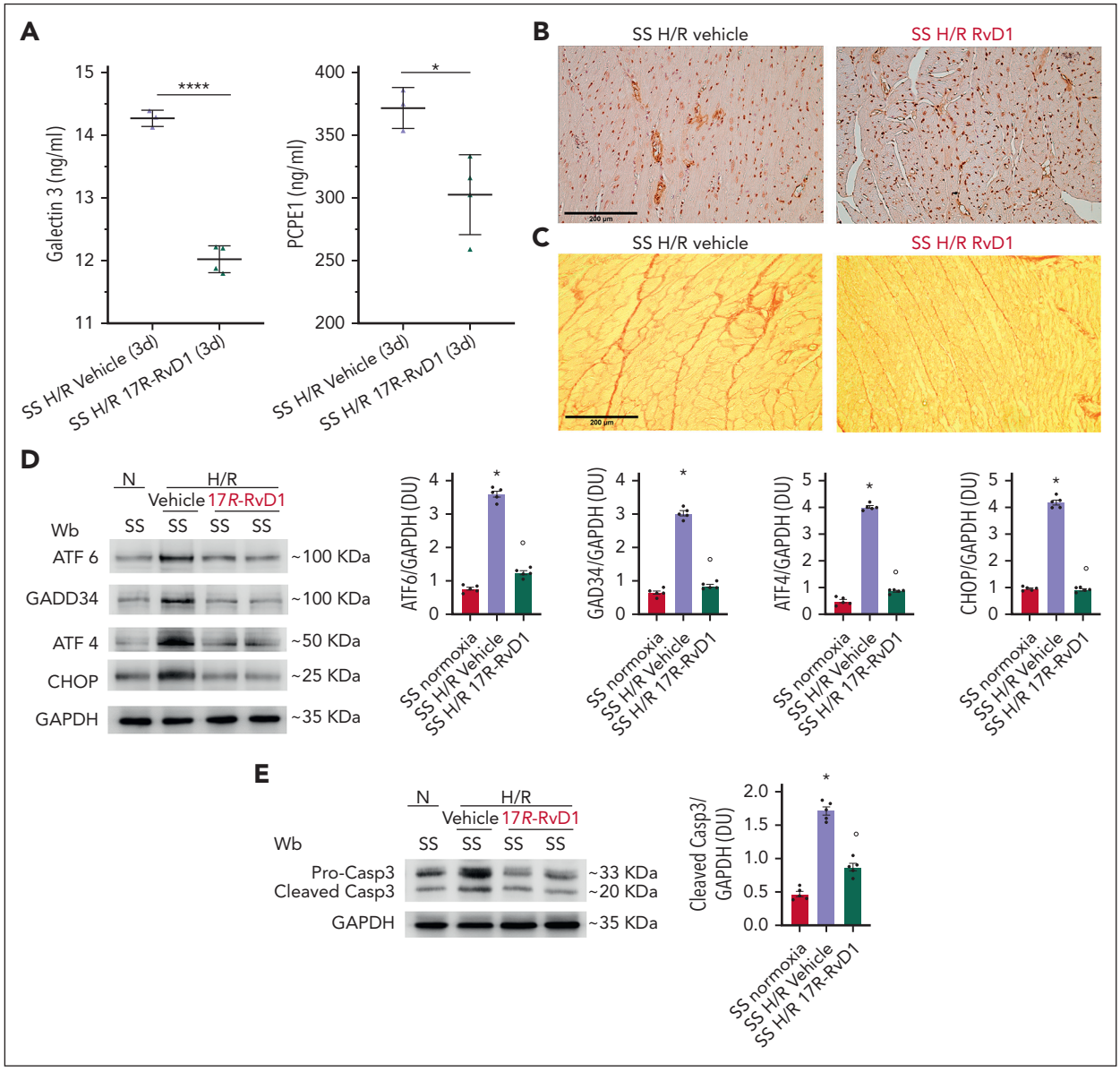

Figure 7. In sickle cell mice, 17R-RvD1 reduces proangiogenic signaling, prevents H/R-induced ER stress, and protects against proapoptotic H/R-induced signature. (A) Serum Gal-3 (left) and procollagen C-proteinase enhancer-1 (PCPE1) in SS mice treated with either vehicle or 17R-RvD1 at 3 days after H/R stress. Data are presented as mean ± SEM (n = 3-4). *P < .05; ***P < .005 (by unpaired t test, with Welch correction). a-SMA (B) and Picrosirius Red (C) staining in cardiac slices from SS mice treated with either vehicle or 17R-RvD1 at 3 days after H/R stress. (D) Immunoblot analysis using specific antibodies against ATF6, GADD34, ATF4, and CHOP in the hearts of AA and SS mice under normoxia, treated with vehicle or 17R-RvD1 (100 ng), and exposed to H/R: hypoxia (8% oxygen; 10 hours), followed by reoxygenation (21% oxygen; 3 hours). One representative gel from 4 gels with similar results is shown; 75 μg/μL of protein loaded on an 11% T, 2.5% C polyacrylamide gel. Glyceraldehyde 3-phosphate dehydrogenase (GAPDH) serves as protein loading control. Densitometric analysis of immunoblots is shown (right). Data are presented as means ± SEM (n = 4). *P < .05 (compared with normoxia); °P < .05 (compared with vehicle-treated mice by 1-way ANOVA). (E) Immunoblot analysis using specific antibodies against caspase-3 in the hearts of AA and SS mice under normoxia, treated with vehicle or 17R-RvD1 (100 ng), and exposed to H/R: hypoxia (8% oxygen; 10 hours), followed by reoxygenation (21% oxygen; 3 hours). One representative gel from 4 gels with similar results is shown; 75 μg/μL of protein loaded on an 11% T, 2.5% C polyacrylamide gel. GAPDH serves as protein loading control. Densitometric analysis of immunoblots is shown (lower). Data are presented as means ± SEM (n = 4). *P < .05 (compared with normoxia). °P < .05 (compared with vehicle-treated mice by 1-way ANOVA). Wb, Western blot.

suppression of miR-16, which regulates pathways involved in apoptosis, inflammation, and cardiac damage[80]; and (2) the downregulation of heart expression of proinflammatory and profibrotic cytokines, such as IL-1b and IL-18, downstream of inflammasome signaling in 17R-RvD1–treated SS mice exposed to H/R. Although the molecular mechanisms underlying miRNA regulation are still poorly defined, initial studies indicate that some miRNAs can be upregulated or downregulated through NF-κB signaling pathways by Rvs, including RvD1 and RvD2.[81,82] Along these lines, the miRNAs found here regulated by 17R-RvD1 have been previously linked to the NF-κB and inflammasome axis, such as miR-25-3p, miR-144-3p, miR-206-3p,[83-85] and miR-208a-3p.[81] Therefore, in SS mice exposed to H/R, our results indicate that 17R-RvD1 regulates select miRNAs through NF-κB and NLRP3 intracellular pathways.

A functional link between NLRP3 inflammasome and UPR system throughout the activation of NF-κB has been recently reported.[86,87] In SS mice, the H/R stress induces a sustained activation of UPR system that causes an accumulation of

oxidized proteins. This might overcome the ability of the UPR system to efficiently operate, switching cells destiny toward apoptosis throughout caspase-3 signaling.[88] Consistently, we found caspase-3 activation in the hearts of SS mice exposed to H/R stress, despite the possible protective effect exerted by ATF6 activation, as reported in models of both HC and acute myocardial infarction.[88] In SS mice exposed to H/R, 17R-RvD1 attenuates ER stress, reduces the activation of UPR system, and rescues the proapoptotic pattern of cardiomyocytes. Our data agree with previous reports in other models of heart diseases, showing the cardio-protective effects of RvD1, which reduces ER stress and, in turn, the overactivation of the UPR system.[22,89] In HC and myocardial postinfarction events, the overactivation of UPR system converges with the activation of FGF-R and PDFGB-R pathways toward profibrotic myocardial remodeling.[90] These intersect miR-206 toward tissue inhibitor of metalloproteinase3 (TIMP3)[91] and synergize with the TGF-β signaling toward Smads, which is also fueled by Gal-3 (Figure 5C). In SS mice exposed to H/R, 17R-RvD1 shifts the inflammatory response to proresolution pattern, preventing the activation of profibrotic pathways and upregulating miR-206. Importantly, 17R-RvD1 also restored normal levels of miR-25 and miR-144, key cardiac function modulators, whose inhibition has been reported to improve cardiac dysfunction in heart failure.[92] The protective effect of 17R-RvD1 against H/R-induced maladaptive remodeling was also supported by (1) the downregulation of heart fibronectin-1 gene expression[56]; (2) the decrease of serum Gal-3 and procollagen C-proteinase enhancer-1; and (3) the reduction of perivascular fibrosis associated with persistent downregulation of ET-1 heart expression. Because ET-1 has been recently reported to induce fibroblast proliferation and to increase a-SMA expression in a dose-dependent manner,[62] we propose that the perivascular fibrosis observed in the hearts of SCD mice after H/R might involve ET-1. Of note, we previously reported that 17R-RvD1 treatment prevented H/R-induced ET-1 expression in different target organs of SCD, showing effects on endothelial dysfunction similar to that of bosentan, an ET-1 receptor antagonist.[23]

In this scenario, the modulation of proangiogenic pathways may be part of the maladaptive signaling in response to H/R stress.[5] In SS mice, treatment with 17R-RvD1 restores miR-206-3p and prevents the activation of HIF-related pro–neoangiogenic pathways, such as VEGF-R phosphorylation and the downregulation of VEGF-A and angiopoietin-2 expression. Thus, in SS mice exposed to H/R, treatment with 17R-RvD1 prevents the activation of both proangiogenic factors (eg, VEGF)[93] and antiangiogenic factors (eg, TGF-β1), breaking the vicious cycle that may contribute to the progression of sickle cell–related cardiovascular disease.[94]

Finally, despite 17R-RvD1 treatment, we observed lack of an effect on miR-18a-5p, 122-5p, 451a, 486-5p, 7a-5p, and 208-3p in SS mice exposed to H/R stress, which might be related to the stage of the mouse heart disease.[3,13,95]

Although our data shed new light on the pathogenesis of sickle cell–related cardiomyopathy, our study has 2 limitations that could be addressed in future studies. The first one is the timeline of the experiments. Here, we focus on an acute setting (H/R stress) with a single dose of 17R-RvD1.[23,96,97] The second limitation concerns the functional measurements by echocardiography, which were performed 3 hours after hypoxia. In future studies, we plan to test a long-term treatment with metabolically resistant benzo-RvD1, which has a longer plasma bioavailability than endogenous 17R-RvD1.[98]

In conclusion, we link, to our knowledge, for the first time, unresolved inflammation and the activation of proinflammatory and profibrotic pathways in the hearts of humanized SS mice exposed to H/R stress, mimicking acute VOCs. Collectively, our results show the value of therapeutic targeting of proresolving events to prevent and treat sickle cell–related cardiovascular disease.

Acknowledgments

The authors thank Charles N. Serhan (Brigham and Women's Hospital and Harvard Medical School, Boston, Massachusetts) for stimulating and fruitful discussion.

This work was supported by Telethon Foundation research grant GPP 20116 and 2020Z22PM7 (L.D.F.).

Authorship

Contributions: E.F. and D.M. contributed to experimental design, conducted experiments, and analyzed data; E.F., A.S., J.C., and V.R. performed immunoblot analyses; M.M. and F.C. performed proteomic analyses, discussed data, and contributed to manuscript writing; M.C. and M.I. performed immunomicroscopy analyses and immunohistochemistry; A.M. performed hematologic analysis and flow cytometric analysis and analyzed data; A.G. and E.T. performed hematoxylin and eosin, Perls and collagen staining and analysis, cardiomyocyte area measurements, and echocardiography; A.G., E.T., and E.G. provided critical review of the manuscript; D.C. and M.H. discussed the experimental design and data and provided critical review of the data; and C.B., A.R., and L.D.F. designed the experiments, analyzed data, and wrote the manuscript.

Conflict-of-interest disclosure: A.G. is a cofounder, shareholder, and scientific adviser of Kither Biotech, a pharmaceutical company developing PI3K inhibitors for respiratory diseases, not in conflict with the content of this article. The remaining authors declare no competing financial interests.

ORCID profiles: D.M., 0000-0002-2149-2855; A.R., 0000-0002-1409-5261; A.M., 0000-0001-5512-5976; F.C., 0000-0002-4648-8107; M.I., 0000-0002-6296-6498; M.C., 0000-0002-4550-8823; A.G., 0000-0002-1193-5296; V.R., 0000-0002-1845-2553; E.G., 0000-0002-2248-1058; C.B., 0000-0001-8192-8713; L.D.F., 0000-0001-7093-777X.

Correspondence: Carlo Brugnara, Department of Laboratory Medicine, Boston Children's Hospital, 300 Longwood Ave, SK-B2-408, Boston, MA 02115; email: carlo.brugnara@childrens.harvard.edu.

Footnotes

Submitted 25 March 2024; accepted 16 January 2025; prepublished online on *Blood* First Edition 10 February 2025. https://doi.org/10.1182/blood.2024024768.

*D.M. and A.R. contributed equally to this study.

Data are available on request from the corresponding author, Lucia De Franceschi (lucia.defranceschi@univr.it). All data related to this study are stored in the Nas Synology DS216se hard disk, located at the University of Verona, and are available on request.

The online version of this article contains a data supplement.

There is a *Blood* Commentary on this article in this issue.

The publication costs of this article were defrayed in part by page charge payment. Therefore, and solely to indicate this fact, this article is hereby marked "advertisement" in accordance with 18 USC section 1734.

REFERENCES

1. Hebbel RP. The systems biology-based argument for taking a bold step in chemoprophylaxis of sickle vasculopathy. *Am J Hematol*. 2009;84(9):543-545.
2. Sachdev V, Machado RF, Shizukuda Y, et al. Diastolic dysfunction is an independent risk factor for death in patients with sickle cell disease. *J Am Coll Cardiol*. 2007;49(4):472-479.
3. Gladwin MT. Cardiovascular complications and risk of death in sickle-cell disease. *Lancet*. 2016;387(10037):2565-2574.
4. Niss O, Quinn CT, Lane A, et al. Cardiomyopathy with restrictive physiology in sickle cell disease. *JACC Cardiovasc Imaging*. 2016;9(3):243-252.
5. Sachdev V, Rosing DR, Thein SL. Cardiovascular complications of sickle cell disease. *Trends Cardiovasc Med*. 2021;31(3):187-193.
6. Bakeer N, James J, Roy S, et al. Sickle cell anemia mice develop a unique cardiomyopathy with restrictive physiology. *Proc Natl Acad Sci U S A*. 2016;113(35):E5182-E5191.
7. Gupta A, Fei YD, Kim TY, et al. IL-18 mediates sickle cell cardiomyopathy and ventricular arrhythmias. *Blood*. 2021;137(9):1208-1218.
8. Carbone S, Lee PJ, Mauro AG, et al. Interleukin-18 mediates cardiac dysfunction induced by western diet independent of obesity and hyperglycemia in the mouse. *Nutr Diabetes*. 2017;7(4):e258.
9. Wagdy R, Assem H, Abd-Elmohsen AM, Fata A, Gendy WE, Gaber M. Altered ventricular longitudinal strain in children with sickle cell disease: role of TGF-beta and IL-18. *Pediatr Blood Cancer*. 2024;71(1):e30762.
10. de Freitas Dutra V, Leal VNC, Fernandes FP, Souza CRL, Figueiredo MS, Pontillo A. Genetic contribution and functional impairment of inflammasome in sickle cell disease. *Cytokine*. 2022;149:155717.
11. Niss O, Detterich J, Wood JC, et al. Early initiation of disease-modifying therapy can impede or prevent diffuse myocardial fibrosis in sickle cell anemia. *Blood*. 2022;140(11):1322-1324.
12. Rai P, Niss O, Malik P. A reappraisal of the mechanisms underlying the cardiac complications of sickle cell anemia. *Pediatr Blood Cancer*. 2017;64:e26607.
13. Niss O, Fleck R, Makue F, et al. Association between diffuse myocardial fibrosis and diastolic dysfunction in sickle cell anemia. *Blood*. 2017;130(2):205-213.
14. Fredman G, Spite M. Specialized pro-resolving mediators in cardiovascular diseases. *Mol Aspects Med*. 2017;58:65-71.
15. Kain V, Ingle KA, Colas RA, et al. Resolvin D1 activates the inflammation resolving response at splenic and ventricular site following myocardial infarction leading to improved ventricular function. *J Mol Cell Cardiol*. 2015;84:24-35.
16. Halade GV, Lee DH. Inflammation and resolution signaling in cardiac repair and heart failure. *EBioMedicine*. 2022;79:103992.
17. Prabhu SD, Frangogiannis NG. The biological basis for cardiac repair after myocardial infarction: from inflammation to fibrosis. *Circ Res*. 2016;119(1):91-112.
18. Li W, Shepherd HM, Terada Y, et al. Resolvin D1 prevents injurious neutrophil swarming in transplanted lungs. *Proc Natl Acad Sci U S A*. 2023;120(31):e2302938120.
19. Gobbetti T, Coldewey SM, Chen J, et al. Nonredundant protective properties of FPR2/ALX in polymicrobial murine sepsis. *Proc Natl Acad Sci U S A*. 2014;111(52):18685-18690.
20. Diaz Del Campo LS, Garcia-Redondo AB, Rodriguez C, et al. Resolvin D2 attenuates cardiovascular damage in angiotensin II-induced hypertension. *Hypertension*. 2023;80(1):84-96.
21. Halade GV, Kain V, Serhan CN. Immune responsive resolvin D1 programs myocardial infarction-induced cardiorenal syndrome in heart failure. *FASEB J*. 2018;32(7):3717-3729.
22. Wang M, Liu M, Zhang J, et al. Resolvin D1 protects against sepsis-induced cardiac injury in mice. *Biofactors*. 2020;46(5):766-776.
23. Matte A, Recchiuti A, Federti E, et al. Resolution of sickle cell disease-associated inflammation and tissue damage with 17R-resolvin D1. *Blood*. 2019;133(3):252-265.
24. Kalish BT, Matte A, Andolfo I, et al. Dietary omega-3 fatty acids protect against vasculopathy in a transgenic mouse model of sickle cell disease. *Haematologica*. 2015;100(7):870-880.
25. Rossato P, Federti E, Matte A, et al. Evidence of protective effects of recombinant ADAMTS13 in a humanized model of sickle cell disease. *Haematologica*. 2022;107(11):2650-2660.
26. Kasztan M, Fox BM, Lebensburger JD, et al. Hyperfiltration predicts long-term renal outcomes in humanized sickle cell mice. *Blood Adv*. 2019;3(9):1460-1475.
27. Beckman JD, Abdullah F, Chen C, et al. Endothelial TLR4 expression mediates vaso-occlusive crisis in sickle cell disease. *Front Immunol*. 2020;11:613278.
28. Ansari J, Senchenkova EY, Vital SA, et al. Targeting the AnxA1/Fpr2/ALX pathway regulates neutrophil function, promoting thromboinflammation resolution in sickle cell disease. *Blood*. 2021;137(11):1538-1549.
29. Tang H, Liu Y, Yan C, Petasis NA, Serhan CN, Gao H. Protective actions of aspirin-triggered (17R) resolvin D1 and its analogue, 17R-hydroxy-19-para-fluorophenoxy-resolvin D1 methyl ester, in C5a-dependent IgG immune complex-induced inflammation and lung injury. *J Immunol*. 2014;193(7):3769-3778.
30. Levy ES, Kim AS, Werlin E, et al. Tissue factor targeting peptide enhances nanoparticle binding and delivery of a synthetic specialized pro-resolving lipid mediator to injured arteries. *JVS Vasc Sci*. 2023;4:100126.
31. Norling LV, Headland SE, Dalli J, et al. Proresolving and cartilage-protective actions of resolvin D1 in inflammatory arthritis. *JCI Insight*. 2016;1(5):e85922.
32. Federti E, Matte A, Recchiuti A, et al. In humanized sickle cell mice, imatinib protects against sickle cell-related injury. *Hemasphere*. 2023;7(3):e848.
33. Vinchi F, De Franceschi L, Ghigo A, et al. Hemopexin therapy improves cardiovascular function by preventing heme-induced endothelial toxicity in mouse models of hemolytic diseases. *Circulation*. 2013;127(12):1317-1329.
34. Yue Z, Chen J, Lian H, et al. PDGFR-beta signaling regulates cardiomyocyte proliferation and myocardial regeneration. *Cell Rep*. 2019;28(4):966-978.e964.
35. Gallini R, Lindblom P, Bondjers C, Betsholtz C, Andrae J. PDGF-A and PDGF-B induces cardiac fibrosis in transgenic mice. *Exp Cell Res*. 2016;349(2):282-290.
36. Dalle Carbonare L, Matte A, Valenti MT, et al. Hypoxia-reperfusion affects osteogenic lineage and promotes sickle cell bone disease. *Blood*. 2015;126(20):2320-2328.
37. Sabaa N, de Franceschi L, Bonnin P, et al. Endothelin receptor antagonism prevents hypoxia-induced mortality and morbidity in a mouse model of sickle-cell disease. *J Clin Investig*. 2008;118(5):1924-1933.
38. Fox BM, Kasztan M. Endothelin receptor antagonists in sickle cell disease: A promising new therapeutic approach. *Life Sci*. 2016;159:15-19.
39. Leask A. Getting to the heart of the matter: new insights into cardiac fibrosis. *Circ Res*. 2015;116(7):1269-1276.
40. Amiri F, Ko EA, Javeshghani D, Reudelhuber TL, Schiffrin EL. Deleterious combined effects of salt-loading and endothelial cell restricted endothelin-1 overexpression on blood pressure and vascular function in mice. *J Hypertens*. 2010;28(6):1243-1251.
41. Amiri F, Virdis A, Neves MF, et al. Endothelium-restricted overexpression of human endothelin-1 causes vascular remodeling and endothelial dysfunction. *Circulation*. 2004;110(15):2233-2240.
42. Ammarguellat F, Larouche I, Schiffrin EL. Myocardial fibrosis in DOCA-salt hypertensive rats: effect of endothelin ET(A) receptor antagonism. *Circulation*. 2001;103(2):319-324.
43. Sandanger O, Ranheim T, Vinge LE, et al. The NLRP3 inflammasome is up-regulated in cardiac fibroblasts and mediates myocardial ischaemia-reperfusion injury. *Cardiovasc Res*. 2013;99(1):164-174.
44. MacKenzie B, Korfei M, Henneke I, et al. Increased FGF1-FGFRc expression in idiopathic pulmonary fibrosis. *Respir Res*. 2015;16(1):83.
45. Wahlquist C, Jeong D, Rojas-Munoz A, et al. Inhibition of miR-25 improves cardiac

contractility in the failing heart. *Nature*. 2014; 508(7497):531-535.

46. Takada S, Maekawa S, Furihata T, et al. Succinyl-CoA-based energy metabolism dysfunction in chronic heart failure. *Proc Natl Acad Sci U S A*. 2022;119(41): e2203628119.

47. Al-Hasani J, Sens-Albert C, Ghosh S, et al. Zyxin protects from hypertension-induced cardiac dysfunction. *Cell Mol Life Sci*. 2022; 79(2):93.

48. Zhao G, Jeoung NH, Burgess SC, et al. Overexpression of pyruvate dehydrogenase kinase 4 in heart perturbs metabolism and exacerbates calcineurin-induced cardiomyopathy. *Am J Physiol Heart Circ Physiol*. 2008;294(2):H936-H943.

49. Fassett J, Xu X, Kwak D, et al. Adenosine kinase attenuates cardiomyocyte microtubule stabilization and protects against pressure overload-induced hypertrophy and LV dysfunction. *J Mol Cell Cardiol*. 2019;130: 49-58.

50. Cuthbert KD, Dyck JR. Malonyl-CoA decarboxylase is a major regulator of myocardial fatty acid oxidation. *Curr Hypertens Rep*. 2005;7(6):407-411.

51. Madrigal-Matute J, Lindholt JS, Fernandez-Garcia CE, et al. Galectin-3, a biomarker linking oxidative stress and inflammation with the clinical outcomes of patients with atherothrombosis. *J Am Heart Assoc*. 2014; 3(4):e000785.

52. Cowling RT, Kupsky D, Kahn AM, Daniels LB, Greenberg BH. Mechanisms of cardiac collagen deposition in experimental models and human disease. *Transl Res*. 2019;209: 138-155.

53. de Boer RA, De Keulenaer G, Bauersachs J, et al. Towards better definition, quantification and treatment of fibrosis in heart failure. A scientific roadmap by the Committee of Translational Research of the Heart Failure Association (HFA) of the European Society of Cardiology. *Eur J Heart Fail*. 2019;21(3): 272-285.

54. Fredman G, Li Y, Dalli J, Chiang N, Serhan CN. Self-limited versus delayed resolution of acute inflammation: temporal regulation of pro-resolving mediators and microRNA. *Sci Rep*. 2012;2:639.

55. Sergienko NM, Donner DG, Delbridge LMD, McMullen JR, Weeks KL. Protein phosphatase 2A in the healthy and failing heart: new insights and therapeutic opportunities. *Cell Signal*. 2022;91:110213.

56. Valiente-Alandi I, Potter SJ, Salvador AM, et al. Inhibiting fibronectin attenuates fibrosis and improves cardiac function in a model of heart failure. *Circulation*. 2018;138(12): 1236-1252.

57. Hiram R, Xiong F, Naud P, et al. The inflammation-resolution promoting molecule resolvin-D1 prevents atrial proarrhythmic remodelling in experimental right heart disease. *Cardiovasc Res*. 2021;117(7): 1776-1789.

58. Meng XM, Nikolic-Paterson DJ, Lan HY. TGF-beta: the master regulator of fibrosis. *Nat Rev Nephrol*. 2016;12(6):325-338.

59. Kessler-Icekson G, Schlesinger H, Freimann S, Kessler E. Expression of procollagen C-proteinase enhancer-1 in the remodeling rat heart is stimulated by aldosterone. *Int J Biochem Cell Biol*. 2006; 38(3):358-365.

60. Hermida N, Markl A, Hamelet J, et al. HMGCoA reductase inhibition reverses myocardial fibrosis and diastolic dysfunction through AMP-activated protein kinase activation in a mouse model of metabolic syndrome. *Cardiovasc Res*. 2013;99(1): 44-54.

61. Shah SJ, Kitzman DW, Borlaug BA, et al. Phenotype-specific treatment of heart failure with preserved ejection fraction: a multiorgan roadmap. *Circulation*. 2016;134(1):73-90.

62. Duangrat R, Parichatikanond W, Likitnukul S, Mangmool S. Endothelin-1 induces cell proliferation and myofibroblast differentiation through the ET(A)R/G(alphaq)/ERK signaling pathway in human cardiac fibroblasts. *Int J Mol Sci*. 2023;24(5):4475.

63. Rodriguez-Pascual F, Busnadiego O, Gonzalez-Santamaria J. The profibrotic role of endothelin-1: is the door still open for the treatment of fibrotic diseases? *Life Sci*. 2014; 118(2):156-164.

64. Crea F, Camici PG, Bairey Merz CN. Coronary microvascular dysfunction: an update. *Eur Heart J*. 2014;35(17):1101-1111.

65. Frangogiannis NG. Matricellular proteins in cardiac adaptation and disease. *Physiol Rev*. 2012;92(2):635-688.

66. Dickhout JG, Carlisle RE, Austin RC. Interrelationship between cardiac hypertrophy, heart failure, and chronic kidney disease: endoplasmic reticulum stress as a mediator of pathogenesis. *Circ Res*. 2011; 108(5):629-642.

67. Tanjore H, Lawson WE, Blackwell TS. Endoplasmic reticulum stress as a pro-fibrotic stimulus. *Biochim Biophys Acta*. 2013; 1832(7):940-947.

68. Zhang G, Wang X, Gillette TG, Deng Y, Wang ZV. Unfolded protein response as a therapeutic target in cardiovascular disease. *Curr Top Med Chem*. 2019;19(21): 1902-1917.

69. Liu Z, Zhang Y, Tang Z, et al. Matrine attenuates cardiac fibrosis by affecting ATF6 signaling pathway in diabetic cardiomyopathy. *Eur J Pharmacol*. 2017;804: 21-30.

70. Li J, Cai SX, He Q, et al. Intravenous miR-144 reduces left ventricular remodeling after myocardial infarction. *Basic Res Cardiol*. 2018;113(5):36.

71. Liu J, Sun F, Wang Y, et al. Suppression of microRNA-16 protects against acute myocardial infarction by reversing beta2-adrenergic receptor down-regulation in rats. *Oncotarget*. 2017;8(12):20122-20132.

72. Zeng N, Wen YH, Pan R, et al. Dickkopf 3: a novel target gene of miR-25-3p in promoting fibrosis-related gene expression in myocardial fibrosis. *J Cardiovasc Transl Res*. 2021;14(6):1051-1062.

73. Song L, Lin C, Gong H, et al. miR-486 sustains NF-kappaB activity by disrupting multiple NF-kappaB-negative feedback loops. *Cell Res*. 2013;23(2):274-289.

74. Doebele C, Bonauer A, Fischer A, et al. Members of the microRNA-17-92 cluster exhibit a cell-intrinsic antiangiogenic function in endothelial cells. *Blood*. 2010;115(23): 4944-4950.

75. Stahlhut C, Suarez Y, Lu J, Mishima Y, Giraldez AJ. miR-1 and miR-206 regulate angiogenesis by modulating VegfA expression in zebrafish. *Development*. 2012; 139(23):4356-4364.

76. Zhong Y, Yu X, Li X, Zhou H, Wang Y. Augmented early aged neutrophil infiltration contributes to late remodeling post myocardial infarction. *Microvasc Res*. 2022; 139:104268.

77. Norling LV, Dalli J, Flower RJ, Serhan CN, Perretti M. Resolvin D1 limits polymorphonuclear leukocyte recruitment to inflammatory loci: receptor-dependent actions. *Arterioscler Thromb Vasc Biol*. 2012; 32(8):1970-1978.

78. Ma Y, Yabluchanskiy A, Iyer RP, et al. Temporal neutrophil polarization following myocardial infarction. *Cardiovasc Res*. 2016; 110(1):51-61.

79. Mattoscio D, Isopi E, Lamolinara A, et al. Resolvin D1 reduces cancer growth stimulating a protective neutrophil-dependent recruitment of anti-tumor monocytes. *J Exp Clin Cancer Res*. 2021; 40(1):129.

80. Toro R, Perez-Serra A, Mangas A, et al. miR-16-5p suppression protects human cardiomyocytes against endoplasmic reticulum and oxidative stress-induced injury. *Int J Mol Sci*. 2022;23(3):1036.

81. Recchiuti A, Krishnamoorthy S, Fredman G, Chiang N, Serhan CN. MicroRNAs in resolution of acute inflammation: identification of novel resolvin D1-miRNA circuits. *FASEB J*. 2011;25(2):544-560.

82. Croasdell A, Thatcher TH, Kottmann RM, et al. Resolvins attenuate inflammation and promote resolution in cigarette smoke-exposed human macrophages. *Am J Physiol Lung Cell Mol Physiol*. 2015;309(8): L888-L901.

83. Luo XY, Ying JH, Wang QS. miR-25-3p ameliorates SAE by targeting the TLR4/NLRP3 axis. *Metab Brain Dis*. 2022;37(6): 1803-1813.

84. Kim HJ, Kim IS, Lee SG, et al. MiR-144-3p is associated with pathological inflammation in patients infected with Mycobacteroides abscessus. *Exp Mol Med*. 2021;53(1): 136-149.

85. Chen M, Zhang J, Huang H, Wang Z, Gao Y, Liu J. miRNA-206-3p alleviates LPS-induced

acute lung injury via inhibiting inflammation and pyroptosis through modulating TLR4/NF-kappaB/NLRP3 pathway. *Sci Rep*. 2024;14(1):11860.

86. Yarmohammadi F, Hayes AW, Karimi G. Possible protective effect of resolvin D1 on inflammation in atrial fibrillation: involvement of ER stress mediated the NLRP3 inflammasome pathway. *Naunyn-Schmiedebergs Arch Pharmacol*. 2021;394(8):1613-1619.

87. Chen X, Guo X, Ge Q, Zhao Y, Mu H, Zhang J. ER stress activates the NLRP3 inflammasome: a novel mechanism of atherosclerosis. *Oxid Med Cell Longev*. 2019;2019:3462530.

88. Glembotski CC. Roles for ATF6 and the sarco/endoplasmic reticulum protein quality control system in the heart. *J Mol Cell Cardiol*. 2014;71:11-15.

89. Wang M, Zhang J, Zhao M, et al. Resolvin D1 attenuates doxorubicin-induced cardiotoxicity by inhibiting inflammation, oxidative and endoplasmic reticulum stress. *Front Pharmacol*. 2021;12:749899.

90. Liu G, Ma C, Yang H, Zhang PY. Transforming growth factor beta and its role in heart disease. *Exp Ther Med*. 2017;13(5):2123-2128.

91. Limana F, Esposito G, D'Arcangelo D, et al. HMGB1 attenuates cardiac remodelling in the failing heart via enhanced cardiac regeneration and miR-206-mediated inhibition of TIMP-3. *PLoS One*. 2011;6(6):e19845.

92. Yuan X, Pan J, Wen L, et al. MiR-144-3p enhances cardiac fibrosis after myocardial infarction by targeting PTEN. *Front Cell Dev Biol*. 2019;7:249.

93. Jin Y, Arita M, Zhang Q, et al. Anti-angiogenesis effect of the novel anti-inflammatory and pro-resolving lipid mediators. *Investig Ophthalmol Vis Sci*. 2009;50(10):4743-4752.

94. Yang X, Cheng K, Wang LY, Jiang JG. The role of endothelial cell in cardiac hypertrophy: Focusing on angiogenesis and intercellular crosstalk. *Biomed Pharmacother*. 2023;163:114799.

95. Damy T, Bodez D, Habibi A, et al. Haematological determinants of cardiac involvement in adults with sickle cell disease. *Eur Heart J*. 2016;37(14):1158-1167.

96. Hong S, Porter TF, Lu Y, Oh SF, Pillai PS, Serhan CN. Resolvin E1 metabolome in local inactivation during inflammation-resolution. *J Immunol*. 2008;180(5):3512-3519.

97. Sun YP, Oh SF, Uddin J, et al. Resolvin D1 and its aspirin-triggered 17R epimer. Stereochemical assignments, anti-inflammatory properties, and enzymatic inactivation. *J Biol Chem*. 2007;282(13):9323-9334.

98. Kim AS, Werlin EC, Kagaya H, et al. 17R/S-Benzo-RvD1, a synthetic resolvin D1 analogue, attenuates neointimal hyperplasia in a rat model of acute vascular injury. *PLoS One*. 2022;17(2):e0264217.